Materials Science & Engineering A 672 (2016) 59–64

Contents lists available at ScienceDirect

Materials Science & Engineering A

journal homepage: www.elsevier.com/locate/msea

New measurement technique of ductility curve for ductility-dip cracking susceptibility in Alloy 690 welds

Kota Kadoi [a,*], Takanori Uegaki [a,1], Kenji Shinozaki [a], Motomichi Yamamoto [a]

[a] Graduate School of Engineering, Hiroshima University, 1-4-1 Kagamiyama, Higashi-Hiroshima, Hiroshima 739-8527, Japan

ARTICLE INFO

Article history:
Received 7 April 2016
Received in revised form
17 June 2016
Accepted 22 June 2016
Available online 23 June 2016

Keywords:
Ductility dip cracking
Hot tensile test
Nickel-based alloy
High temperature ductility curve
In situ observation

ABSTRACT

The coupling of a hot tensile test with a novel in situ observation technique using a high-speed camera was investigated as a high-accuracy quantitative evaluation method for ductility-dip cracking (DDC) susceptibility. Several types of Alloy 690 filler wire were tested in this study owing to its susceptibility to DDC. The developed test method was used to directly measure the critical strain for DDC and high temperature ductility curves with a gauge length of 0.5 mm. Minimum critical strains of 1.3%, 4.0%, and 3.9% were obtained for ERNiCrFe-7, ERNiCrFe-13, and ERNiCrFe-15, respectively. The DDC susceptibilities of ERNiCrFe-13 and ERNiCrFe-15 were nearly the same and quite low compared with that of ERNiCrFe-7. This was likely caused by the tortuosity of the grain boundaries arising from the niobium content of around 2.5% in the former samples. Besides, ERNiCrFe-13 and ERNiCrFe-15 indicated higher minimum critical strains even though these specimens include higher content of sulfur and phosphorus than ERNiCrFe-7. Thus, containing niobium must be more effective to improve the susceptibility compared to sulfur and phosphorous in the alloy system.

1. Introduction

Ductility-dip cracking (DDC) is a type of weld hot cracking that initiates in the solid state at above 50% of the melting point [1,2]. The cracks occur at grain boundaries free of liquid phases, and often occur in austenitic metals such as Cr-Ni type stainless steels and nickel-based alloys. The size of such cracks is quite small (<1 mm), which makes it difficult to detect them during inspection and means that prevention of crack occurrence is required. It is known that DDC occurs by an intergranular embrittlement that corresponds to segregation of impurity elements such as sulfur and phosphorus, and microconstituents [2–4]. However, the detailed mechanism of DDC is still under discussion.

DDC susceptibility has been quantified using high temperature ductility curves that show the relationship between temperature and critical strain for crack occurrence. The ductility-dip temperature range and minimum critical strain are important factors in DDC susceptibility. Thus, the strain and the temperature at which crack initiation occurs must be measured with high precision. Several test methods have been used to investigate DDC susceptibility, including the trans-Varestraint test [1–4] and strain-to-fracture test [5,6]. The trans-Varestraint test can measure ductility-dip temperature range but cannot measure the local strain required for DDC to occur within the ductility-dip temperature range. Besides, it is often difficult to distinguish DDC from liquation cracking because the ductility-dip temperature range is very close to the temperature range of liquation cracking [2]. The strain-to-fracture test, developed by Nissley et al., enables a ductility curve to be obtained by controlling the test temperature and measuring the strain for DDC initiation using a Gleeble tester [5,6]. However, the measured strain must be far from the true critical strain contributing to DDC initiation because the 4 mm gauge length typically used for the strain measurement is too long compared with the size of the crack. Additionally, the strain is measured at room temperature using a binocular microscope with a magnification of around 30 [5,6]. For more detailed prediction and better prevention of DDC occurrence, a quantitative value such as the critical strain must be measured with higher precision. Therefore, a test method that makes it possible to directly measure the local critical strain at high temperature must be developed so that the mechanism of DDC and DDC susceptibility can be quantitatively determined in greater detail.

The aim of this work was to establish a highly accurate quantitative evaluation method for DDC susceptibility. The coupling of a hot tensile test with a developed in situ observation technique using a high-speed camera was carried out to measure the critical strain for crack initiation directly during high temperature ductility curve measurement. Several types of Alloy 690 filler wire were used in this study because this alloy is known to be susceptible to DDC.

* Corresponding author.
E-mail address: kadoi@hiroshima-u.ac.jp (K. Kadoi).
[1] Present address: Hitachi Construction Machinery Co., Ltd.

http://dx.doi.org/10.1016/j.msea.2016.06.062
0921-5093/

2. Experimental procedure

2.1. Materials used

Table 1 shows the chemical compositions of the base material and filler wires used in this work. SUS304L ($280 \times 50 \times 5$ mm^3) was used as the base material for specimen fabrication. ERNiCrFe-7 (AWS standard, ϕ1.1 mm), ERNiCrFe-13 (AWS standard, ϕ1.1 mm) and ERNiCrFe-15 (AWS standard, ϕ1.2 mm) were used as the Alloy 690 filler wires.

2.2. Specimen fabrication

The chemical composition of the evaluation area of the specimens was required to be identical to that of the filler wires. A hot-wire laser welding process was employed for specimen fabrication owing to its advantages of controllable deposit ratio and reduced dilution of the base material [7,8]. Batch processes were carried out in order of buttering welding, butt welding, gas tungsten arc (GTA) bead on welding, and cutting out of specimens, as shown in Fig. 1. Table 2 shows the welding conditions used during specimen fabrication. A fibre laser was employed as the heat source. The laser spot diameter was 7.0 mm, controlled by defocusing from a focal distance of the laser beam. The wire current was adjusted corresponding to the type, the diameter, and the feeding speed of the wire.

In the first step (Fig. 1(a)), buttering welding was carried out on the SUS304L base material. Next, the welded part was machined with a bevel angle of 10° (Fig. 1(b)). Butt welding was then performed on the machined samples with a set groove width of 4.2 mm (Fig. 1(c)). As a final step, GTA bead on welding under welding conditions (welding current: 150 A, welding speed: 0.08 m/min) similar to those used in practical welding was carried out to give the area evaluated for cracking susceptibility a suitable welding heat history (Fig. 1(d)). The dilution ratio of SUS304L into the buttering weld metal was around 1%, and the ratio of the buttering weld metal to the butt weld metal was 20–30%. Thus, the final dilution ratio of SUS304L in the evaluated area in the sample was less than 0.3%. Finally, a $2 \times 4 \times 112$ mm^3 specimen was cut from the surface of the sample for the hot tensile test (Fig. 1(e)).

Preliminary tests revealed that DDC often initiated near the centreline of the GTA weld bead. Thus, 28 gauge marks were placed 0.5 mm apart within a 3×15 mm^2 area around the centreline on the specimen using a Vickers indenter. The centreline was identified by electrolytic etching using 10% oxalic acid.

2.3. Hot tensile test with in situ observation technique

Fig. 2 shows the experimental set-up for the hot tensile test and in situ observation system. The set-up consisted of a high frequency induction heater, a tensile tester, a tensile test jig, and a high-speed camera. The specimen was fixed on the jig inside a quartz tube through which Ar gas was flowed to avoid oxidation of the specimen during the test. An R-type thermocouple (ϕ 0.5 mm) was attached to the back side of the specimen for the control and measurement of its temperature during the test. The high-speed camera was placed on a 3-axis table to control the test observation position. A metal halide lamp was used to obtain a clear image.

The specimen was heated up to the chosen test temperature for 30 s from the start of heating and held at the temperature. The induction heating program was set to prevent overshoot and hunting. The tensile test was started with a cross head speed of 0.1 mm/s 30 s after the start of heating and was continued for the selected test time, as shown in Fig. 2c). The test temperature was varied from 700 to 1050 °C, which has been reported as the ductility-dip temperature range of Ni-based alloys [1,2]. The applied strain was controlled by changing the test time. The gauge marks (Vicker's marks) on the specimen were monitored during the hot tensile test using the high-speed camera to directly measure the strain. The measured applied strain was calculated based on the following equation:

$$\varepsilon = (l_1 - l_0)/l_0 \times 100$$

where l_0 is the initial distance between the gauge marks, i.e., 0.5 mm, and l_1 is the distance between the marks after the test. l_0, l_1, and the strain history were measured by tracing the marks in the high speed camera movie using image analysing software.

The surface of the specimen was observed after the test using a

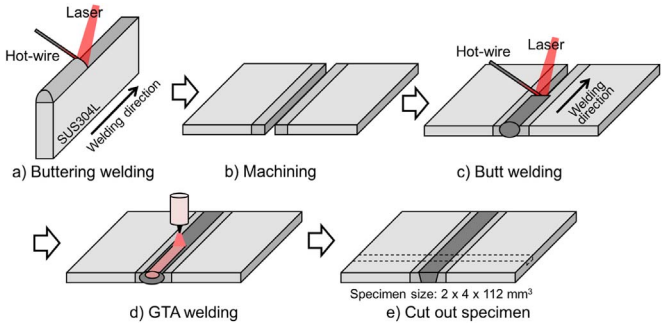

Fig. 1. Schematic illustration of specimen fabrication steps using hot-wire laser welding process.

Table 2
Welding conditions for specimen fabrication.

	Buttering	Butt
Laser power, kW	3.0	3.0
Welding speed, m/min	0.1	0.2
Laser spot diameter, mm	7	7
Laser irradiation angle, deg	5	5
Wire feeding speed, m/min	6.0	7.0
Wire current, A	108–115	126–134
Wire feeding angle, deg	70	70

Table 1
Chemical composition of base material and filler wires (mass%).

	C	Si	Mn	P	S	Ni	Cr	Fe	Mo	Nb	Ti	Al	Cu
SUS304L	0.023	0.62	1.01	0.026	0.008	9.06	18.2	Bal.	–	–	–	–	–
ERNiCrFe-7	0.025	0.13	0.24	0.002	0.001	Bal.	29.23	9.99	0.04	0.01	0.55	0.65	0.02
ERNiCrFe-13	0.023	0.11	0.31	0.004	< 0.0005	Bal.	29.5	8.79	3.51	2.51	0.18	0.13	0.05
ERNiCrFe-15	0.043	0.05	2.97	0.003	0.001	Bal.	27.0	2.55	0.01	2.29	0.30	0.05	0.01